Developing a slip budget for crustal faulting in western Washington: Implications for seismic hazard “

Final Project Summary
Assistance Award 03HQGR0087

Meghan Miller
Department of Geological Sciences
Central Washington University
Ellensburg, WA 98926
509/963-2825 (voice)
509/963-1109 (fax)
meghan@geology.cwu.edu
http//www.geology.edu/facstaff/meghan

Program Element: Elements II
Key Words: GPS-Continuous, GPS Campaign, Regional Modeling, Neotectonics

Investigations Undertaken

NEHRP funded several CWU proposed tasks in FY 2002, including convening the annual PANGA investigator community meeting (which took place in Spring 2003 at CWU), and block modeling of Pacific Northwest GPS vectors derived from the PANGA array to better constrain the crustal faulting rates and slip budgets for western Washington. The grant supported the Master’s thesis of Michael Caron, who defended in 2004. Below we include a brief summary of the funded PANGA investigator meeting, and the follow with a revised manuscript resulting from Michael Caron’s Master’s thesis.

I)PANGA Investigator Meeting:

Two 2-day PANGA investigator community meeting was convened in March of 2003 at the Pacific Geosciences Center in Sydney, BC, and drew 48 attendees. The meeting was highly effective and served their purpose of bringing everybody up to speed on the majority of ongoing, GPS-based tectonics research. The attendees are shown in the following table.

Patricia McCrory	USGS-Menlo	pmccrory@usgs.gov
Meghan Miller	CWU	meghan@geology.cwu.edu
Evelyn Roeloffs	USGS-CVO	evelynr@usgs.gov
Ana Cadena	CWU	ana@geology.cwu.edu
Katrin Hafner	UNAVCO	australis@earthlink.net
Jill Johnson	Seattle	JJOHNS3@co.pierce.wa.us
Walter Szeliga	CWU	walter@geology.cwu.edu
Free		
Andrew Miner	CWU	minera@geology.cwu.edu

Frederick Blume	UNAVCO	blume@unavco.org
Karl Feaux	UNAVCO	kfeaux@unavco.ucar.edu
Sean Willett	UW	tony@ess.washington.edu
Mark Brandon	YALE	mark.brandon@yale.edu
David Verdonck	SUNY	dverdonck@eglab.org
Michael Lisowski	USGS/CVO	mlisowski@usgs.gov
Tony Qamar	UW	swillett@u.washington.edu
David Schmidt	UofO	das@darkwing.uoregon.edu
Ray Weldon	USGS/CVO	ray@newberry.uoregon.edu
Gary Gervelis	LSAW-Seattle	Gary.Gervelis@Seattle.gov
David Steele	WA DNR	dave.steele@wadnr.gov
Robert Maconie	City of Renton	bmaconie@ci.renton.wa.us
David Mencin	Unavco	mencin@unavco.org
Les Olsen	Seattle	lolsen@co.pierce.wa.us
Wayne Thatcher	USGS-Menlo Park	thatcher@usgs.gov
Mike Jackson	UNAVCO	mikej@unavco.ucar.edu
Ray E. Wells	USGS-Seattle	rwells@usgs.gov
Juliet G. Crider	WWU	criderj@cc.wwu.edu
Gary Perasso	NGS-Seattle	Gary.Perasso@noaa.gov
Tim Melbourne	CWU	tim@geology.cwu.edu
Elizabeth Hearn	UBC-Vancouver	ehearn@eos.ubc.ca
Amanda Bustin	PGC (student)	abustin@NRCan.gc.ca
Roy Hyndman	PGC	rhyndman@nrcan.gc.ca
Lisa Wolynec	SEOS (student)	lwolynec@uvic.ca
Herb Dragert	GSC	hdragert@NRCan.gc.ca
Lucinda Leonard	UVIC	lucindal@uvic.ca
Brian Schofield	GSC	bschofield@NRCan.gc.ca
Stephan Mazzotti	GSC	SMazzotti@NRCan.gc.ca
Bert Struik	GSC Vancouver	BStruik@nrcan.gc.ca
Gary Rogers	GSC	rogers@pgc.nrcan.gc.ca
Bird, Allison	GSC	albird@NRCan.gc.ca
Cassidy, John	GSC	jcassidy@NRCan.gc.ca
He, Jianghen	GSC	jhe@NRCan.gc.ca
Hu, Yan	GSC	yhu@NRCan.gc.ca
James, Tom	GSC	tjames@NRCan.gc.ca
Schmidt, Mike	GSC	mschmidt@NRCan.gc.ca
Wang, Kelin	GSC	kwang@NRCan.gc.ca
Weichert, Dieter	GSC	diweiche@NRCan.gc.ca
Wynne, Jane	GSC	jwynne@NRCan.gc.ca
Ele Willoughby	GSC	ewilloug@NRCan.gc.ca
Claire Currie	GSC	ccurrie@NRCan.gc.ca
Ross Chapman	GSC	chapman@uvic.ca

II) Block Modeling of PANGA GPS vectors

Prior to 2001, the velocity field from Puget Sound came from a network of stations which, for the most part, were not on geodetic quality monuments. These stations included a combination of regionally available NGS/other stations and several that have been funded through the NEHRP program. Because of technical issues relating to high precision velocity determinations, not all of these stations were equally valuable. Detailed statistical analyses of the data time series was needed to resolve existing discrepancies and to further minimize systematic errors that affected the data. By contrast, today the time series are now long enough and robust enough to support such studies which simply are not possible from campaign data alone.) With the refined velocities, Caron then generated a kinematically consistent block model for the strain gradient observed across the Puget Lowlands. The first generation of this model included known geologic constraints and the sparse but high precision results from the time series analysis. The model was built in such a way that future modifications can add in the constraints from new geodetic quality stations that were installed in 2003-8, which eventually will number 355 continuous, well-monumented stations.

Here we include a manuscript that we intend to submit to *Bulletin of the Geological Society of America,* based entirely on the Master's thesis of Michael Caron, who was supported of 03HQGR0087.

Geodetically Constrained Estimates of Secular Deformation and Seismic Potential in the Puget Lowland of the Cascadia Fore-arc

Michael Edward Caron

M. Meghan Miller

Marcelo Santillan

ABSTRACT

A fault block model inversion, constrained by Continuous Global Positioning System (CGPS) geodesy from the Pacific Northwest Geodetic Array (PANGA), yields slip rates estimates for faults in the Puget Lowland This approach assumes that, to first order, the GPS-determined velocities result from a combination of kinematically consistent rigid fault block motion and interseismic strain accumulation due to locking of faults along block boundaries. A horizontal north-directed shortening rate of 4.5 to 6 mm per year across the Puget Lowland is indicated. Earthquake recharge intervals were estimated from slip rates as well as moment accumulation considerations and indicate an apparent deficit of M_w 6 or larger earthquakes in the Puget Lowland, due perhaps to an incomplete earthquake catalog or to a lull in a clustered earthquake record.

INTRODUCTION

The Puget Lowland forms one in a series of forearc basins along the Cascadia convergent margin, where the Juan de Fuca plate subducts under western North America (Figure 1). The Juan de Fuca plate, a remnant of the once extensive Farallon plate, is a small oceanic plate embedded in the Pacific – North America transform system between a pair of migrating triple junctions located more than 1,000 kilometers apart. Northward translation of the southern Cascadia forearc results from the three plate interaction (Mazzotti et al., 2002; Miller et al., 2001; Wells and Johnson, 2000) and terminates against a buttress of crystalline rocks in Vancouver Island and the Coast Range of British Columbia. The resulting crustal shortening is accommodated by active west-striking reverse faults that form the boundaries between basins and uplifted blocks within the Puget Lowland. Geophysical data illuminate active fault geometry, but deep glacial erosion, extensive glaciomarine cover, and widespread urbanization obscure young structures, and their slip rate distribution is not well known.

In this study, we derive estimates for slip rates using a block model for crustal faults in the Puget Lowland, inverted from continuous Global Positioning System (CGPS) geodetic constraints provided by the Pacific Northwest Geodetic Array (PANGA). This approach assumes that the annual GPS velocity field results from a combination of kinematically consistent rigid fault block motion and elastic strain accumulation that results from locking of faults along block boundaries. Deformation at a finer spatial scale or better precision than the velocity field can resolve, permanent deformation internal to model fault blocks, as well as time variant deformation throughout the earthquake cycle are assumed to be negligible. The model provides first order fault slip estimates along segments of modeled faults that best describe the GPS velocity field. These results have implications for seismic hazard posed by crustal faults in the populous Puget Lowland area, providing fault slip budgets that describe the roles of individual faults in generating earthquakes. They further bear on the neotectonic framework of the region.

GEOLOGIC SETTING

Northward-directed Cascadia forearc motion of 3 to 7 mm per year (Mazzotti et al., 2002; Miller et al., 2001; Wells and Johnson, 2000) in Cascadia is buttressed against crystalline rocks of Vancouver Island and the Coast Range of British Columbia, and accommodated on west to northwest-striking strike-slip or oblique-slip faults and on typically north-dipping, west-striking reverse faults. The Seattle fault, however, dips towards the south. Some of the key faults in the Puget Lowland include the Doty and Tacoma faults, and the Seattle, South Whidbey Island, and Devils Mountain fault zones (Figure 3). Farther west, the Little River fault bounds the north margin of the Olympic Mountains uplift, and the Leech River and Tofino faults transect Vancouver Island. The disparity in northward translation rates between the forearc and the backarc is likely accommodated along north-striking strike-slip faults such as the Straight Creek fault and its northward continuation, the Fraser fault in British Columbia. The boundary between the forearc and backarc south of the Puget Lowland is enigmatic and may be distributed over numerous short north-striking *en echelon* faults (Miner, 2002b).

The Puget Lowland forms part of a segmented, linear forearc basin extending from Georgia Strait in British Columbia to the Willamette Valley in Oregon. The eastern boundary of the Siletz terrane is hidden beneath thick sediments of the Puget Lowland or by volcanic rocks of the Cascade Range (Trehu et al., 1996). To the north, the South Whidbey Island fault and the Leech River–Tofino faults likely separate Siletzia from older basement rocks (Brocher et al., 2001). In Puget Sound, structural basins are defined by isostatic gravity, aeromagnetic surveys and topography (Figure 4). Mafic rocks of the Siletz terrane, consisting largely of submarine and subaerial basaltic rocks of the lower Eocene Crescent Formation, floor these basins. Up to 10 km of upper Eocene and younger marine sediments and Quaternary glacial sediments fill the basins (Brocher et al., 2000).

During advances of the Pleistocene Cordilleran ice sheet, alpine glaciers from the Canadian Coast Range coalesced and extended to the south into Puget Sound and to the west into the Strait of Juan de Fuca. Superimposed generations of till in southern Puget Sound record five or six advances of the Puget lobe during the late Quaternary (Easterbrook, 1992; Johnson et al., 1999; Thorson, 1996). During the most recent Vashon stade, between about 15,000 B.P and 13,500 B.P., the Puget lobe entirely filled the Puget Lowland between the Cascade Range and the Olympic Mountains to the west, with a lobe of ice exceeding 1 km in depth (Thorson, 1996). Withdrawal of the glacial lobe left the area mantled with extensive Pleistocene glacial drift and associated reworked sediments up to 1,100 m thick (Yount et al., 1985). Thick glacial sediment, deep glacial erosion, and urbanization obscure direct observation of young structural features.

The Puget Lowland displays paleoseismic evidence of moderate to large prehistoric earthquakes along crustal faults. Stratigraphic and geomorphic evidence from coastal marshes and beaches indicate abrupt relative sea level changes due to sudden, localized uplift or subsidence events during the past several thousand years beneath (Bucknam et al., 1997). Evidence of liquefaction and submarine landslides is also locally preserved (Karlin et al., 1995). The paleoseismic record prior to about 6,000 B.P. is masked by a rapid rise in sea level, and extensive glacial erosion and deposition obscure much of the Holocene record. Locally preserved paleoseismic records imply fault slip amount and earthquake moment magnitudes. For example, an estimated M_w 7 earthquake along the Seattle fault in A.D. 900–930 is recorded by 7 m of vertical displacement on beaches at Restoration Point on Bainbridge Island (Bucknam et al., 1992). Paleoseismic studies along the Toe Jam Hill fault on Bainbridge Island shows evidence for at least three earthquakes related to surface ruptures since the recession of the Puget ice lobe about as much as 16,000 years ago (Nelson et al., 2002). At the Snohomish River delta located north of Seattle, the stratigraphic record indicates two to five additional earthquakes within the past 1,200 years (Bourgeois and Johnson, 2001). In general, the paleoseismic records are not complete enough to quantify earthquake recurrence intervals or slip rates, although loose constraints can be inferred for a few faults. The Seattle fault, for example, does not appear to have been affected by a large magnitude earthquake in a 5,500-year period before the large earthquake of A.D. 900–930 (Bucknam et al., 1997).

Limited outcrop mapping, together with subsurface illumination by geophysical methods, allows interpretation of major crustal faults in the Puget Lowland. Subsurface geometry, evolution, and slip rates on individual faults are not well-constrained, however, due largely to poor exposure. To date, inferred slip rates have been based largely on a fragmentary paleoseismic record, such as offsets interpreted from high-resolution seismic-reflection surveys (Johnson et al., 1999) or geologic constraints derived from borings (Johnson et al., 2000).

METHOD

CGPS geodesy provides high precision estimates of surface deformation rates. These rates, taken from average annual station velocities, are used to constrain a kinematically consistent block model of deformation using software developed by Meade and others (2002). In order to enforce the path integral constraint, all blocks are circumscribed by faults, with *a priori* location, strike, dip, and locking depth. Block motion is inverted from the observed GPS velocities simultaneously with the recoverable deformation resulting from fault locking. The latter effect decreases with distance from the fault and thus, where block boundaries lie far from geodetic constraints, the details of locking depth have little direct impact on estimated block motions.

This approach requires several steps: determination of the CGPS velocity field, construction of a block geometry appropriate to the spatial resolution and precision of the velocity field, application of *a priori* constraints, and inversion of the model for block motion and fault-related recoverable deformation. The model simplifies known processes, neglecting permanent deformation within model fault blocks and the variation in deformation rates throughout the earthquake cycle. Nonetheless, the model places first order constraints on fault slip rate and seismic strain accumulation.

GPS Velocity Field

The Pacific Northwest Geodetic Array (PANGA) comprises a network of continuously operating GPS receivers along the Cascadia convergent margin (Miller et al., 2001). PANGA includes stations in a regional U.S. array coordinated by Central Washington University and those of the Western Canada Deformation Array (WCDA) operated by Pacific Geoscience Centre in British Columbia. The CWU Geodesy Laboratory and PANGA Data Analysis Facility carries out daily analyses of PANGA and other regionally available CGPS data using GIPSY/OASIS II software (release 4) from the Jet Propulsion Laboratory (JPL), producing high-precision daily estimates of position and velocity based on time-series over several years (Zumberge et al., 1997). The GPS velocity solutions utilize ITRF 2000 (International Terrestrial Reference Frame), which provides a global reference frame based on the global IGS (International GPS Service) network (Altamimi et al., 2002). Daily positions in the International Terrestrial Reference Frame were determined following Miller et al. (2001) with certain improvements, including application of ambiguity resolution. Annual and semiannual effects were rigorously removed using qrfit, a set of software tools developed at Central Washington University (Szeliga reference- two GRL papers in 2005…). Qrfit removes annual and semiannual atmospheric and solid earth effects (Blewitt et al., 2001), and accounts for steps in the time-series due to antenna or receiver changes as well as tectonic events. Changes in station position over time within the ITRF form the basis for velocity determinations; velocity uncertainties were estimated following Mao et al. ***.

Seventeen stations were used in the transformation of the velocity field from the ITRF 2000 reference frame to GPS-defined North America, with negligible differences compared to previous solutions but with significant improvement in uncertainty as observation history, position estimates, and time series analysis tools have improved.

Finally, a correction was applied to the velocity field to remove estimated elastic deformation due to coupling between Juan de Fuca and North America (Miller et al., 2001). This was necessary because the current version of the block modeling code does not accommodate a complex fault geometry, such as the arched subducting Juan de Fuca plate. In this method, revised Euler vectors for North America and Pacific plates based on a global plate circuit solution (DeMets and Dixon, 1999) propagate to an Euler vector for Juan de Fuca–North America (Miller et al., 2001b). This results in a larger rotation rate for Juan de Fuca relative to North America than previous estimates such at NUVEL 1A (DeMets et al., 1994). Using the three dimensional dislocation model for Cascadia of Fluck et al. (1997), modified to account for slip variation along strike, convergence rates between the forearc and Juan de Fuca are determined iteratively. The elastic strain that accumulates above the Cascadia subduction zone is estimated and subtracted from GPS velocities. The residual velocity field estimates long-term deformation rates including migration of the forearc relative to North America. Appendix 1 lists velocities that constrain the model.

Block Model

The block model uses the approach and Matlab-based software (sp3) of Meade et al., (XXXX). The first step is construction of a crustal block geometry appropriate to the spatial resolution and precision of the velocity field. Each structural block must be fully circumscribed by model fault segments, have at least two GPS constraints for the inversion, and its boundaries should be structures with geodetically resolvable slip rates, appropriate to the precision of the velocity field. Geologic and geophysical data sets were integrated in a GIS in order to define the block geometry in the Puget Lowlands; this is detailed in Caron (2003). All fault segments must connect at the surface; this required extending several faults beyond current mapped extents. The model Seattle fault, for example, extends about 15 km farther along strike than its mapped extent in order to satisfy the requirement for polygon closures.

Once block geometry is defined and closure is achieved, certain *a priori* constraints are required including fault dip and locking depth. While these are not always well resolved from existing geologic and geodetic constraints (see detailed discussion in Caron, 2003), variation within reasonable uncertainty estimates has little effect on inversion results. Variation in fault dip estimates has direct consequences for seismic moment accumulation (discussed below), but does not strongly affect inversion of block motion within uncertainty ranges of several tens of degrees. Similarly, inversion of the block model over locking depths of 10 and 15 km resulted in little variance in calculated slip rates, with differences on individual fault segments generally not exceeding 0.2 mm per year, below the sensitivity of the velocity field. An *a priori* locking depth constraint of 15 km was applied to each crustal fault segment in the block model. The burial depth, which allows for a subsurface upper boundary on fault locking, was not used in our model. Introduced constraints on fault slip rate are also allowed where GPS constraints are insufficient to support the model fault geometry; this option was not needed in our model.

Inversion

The inversion of GPS velocities to constrain block motions and accumulation of elastic deformation near locked fault boundaries uses Matlab-based software developed for this purpose (McClusky et al., 2001; Meade et al., 2002). The method simultaneously estimates block motions and fault slip rates by a weighted least squares inversion of the modified velocity vectors (McClusky et al., 2001). A path integral constraint is applied, which requires kinematic consistency where blocks are assumed rigid and point to point relative motion estimates are independent of path taken and faults crossed. A translation defined by two horizontal velocity components and a rotation rate, defined by an Euler vector, describe horizontal block motions, so that faults bounding blocks have slip rates that may vary along strike. Residual differences between the velocity field constraint and velocities predicted by the model results are minimized.

RESULTS

Inversion of GPS velocities calculates dip-slip and strike-slip rates, as well as tensile opening or closing rates where required for kinematic consistency. Dip-slip rates (shown as the horizontal component of slip, i.e., shortening or extension) and strike-slip rates are summarized for the major west-striking faults in the Puget Lowland in Table 1 (see Figure 3 for fault locations):

Table 1. Modeled Dip-Slip (horizontal component) and Strike-Slip Rates for Major Faults in the Puget Lowland

Fault	Dip	Dip-Slip	Strike-Slip[1]
Doty fault	70° N	1.3 to 4.9 mm reverse	1.3 mm LL to 0.5 mm RL
Tacoma fault	65° N	0.1 mm to 3.8 mm reverse	4.0 mm to 5.0 mm LL
Seattle fault	40° S	1.8 mm to 3.3 mm normal	4.5 mm to 4.9 mm LL
South Whidbey Is. fault	80° N	1.9 mm normal to 4.5 mm reverse	4.3 mm to 6.3 mm LL
Devils Mountain fault	61°N	0.9 mm normal to 9.1 mm reverse	0.3 mm to 3.3 mm RL
Leech River fault	30° N	0.2 mm normal	0.2 mm RL
Little River fault	70° N	2.1 mm normal to 1.3 mm reverse	3.0 mm to 4.5 mm RL

(1) LL = left lateral, RL = right lateral

Figure 3. Key Slip Rates (dip-slip [horizontal component] and strike-slip)

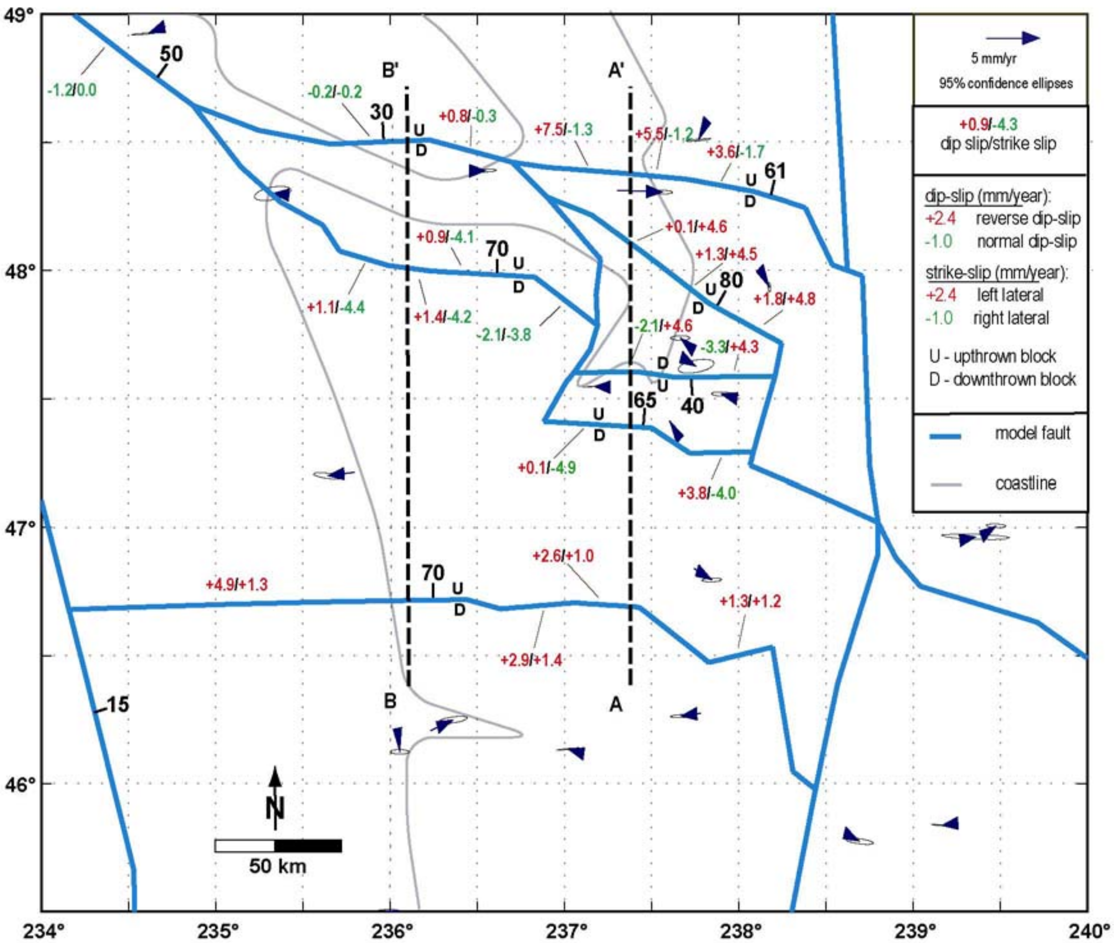

Two north-south transects through Puget Sound along longitude 236.1 ° W and longitude 237.4° W, shown as A-A' and B-B', respectively, on Figure 3, intersect the following model faults, each shown with the horizontal component of dip-slip as summarized in Table 3:

Table 3. Slip Rates for Key Faults (horizontal component of dip-slip)

Fault	**Dip-slip rate (A-A')**	**1σ uncertainty[(1)]**	**Dip-slip rate (B-B')**	**1σ uncertainty[(1)]**
Doty fault	+2.6 mm/year	0.1 mm/year	+4.9 mm/year	0.1 mm/year
Tacoma fault	+0.1 mm/year	0.2 mm/year		
Seattle fault	-2.1 mm/year	0.2 mm/year		
S. Whidbey Is. fault	+0.1 mm/year	0.3 mm/year		
Devils Mountain fault	+5.5 mm/year	0.2mm/year		
Little River fault			+1.4 mm/year	0.1 mm/year
Leech River fault			-0.2 mm/ year	0.1 mm/year
Total:	***+6.2 mm/year***	***± 1.0 mm/year***	***+6.1 mm/year***	***± 0.3 mm/year***

[(1)] uncertainty refers to calculated horizontal component of dip slip uncertainty

The close agreement between the two slip estimates supports the kinematic consistency of inversion and indicates that total N-S shortening across the fore-arc in western Washington is about 6 mm per year. Previous shortening estimates range from about 3 mm per year (Mazzotti et al., 2002) to about 7 mm per year (Miller et al., 2001).

Inversion results in slip rates that are generally sensibly distributed across the active faults of the crustal block model. Most calculated slip rates are robust and vary little with changes in *a priori* constraints such as locking depth. Calculated slip in a few cases may be unstable, however. One such location is the northwestern segment of the South Whidbey Island fault, where the fault is forced to accommodate differences in translation and rotation between a block in the Puget Lowland and a block in the foreland to the west. Known errors in the time-series from GPS station SEAW may also contribute to unrealistic block rotation rates. A review of formal 1σ uncertainties calculated during inversion shows that one of the eastern segments of the model South Whidbey Island fault and the westernmost segment of the model Tacoma fault have dip-slip uncertainties that exceed calculated slip rates. Other uncertainties calculated during inversion do not exceed calculated slip rates and are generally low.

DISCUSSION

Previous slip estimates for the Puget Lowland depend on geologic and geophysical constraints and paleoseismic considerations. Estimated slip rates from identified crustal faults in western Washington, northern Oregon, and southwestern British Columbia provide a comparison with inversion results. Some amilies of faults, with slip distributed among more than one fault strand, such as the Tacoma fault zone, Seattle fault zone, the South Whidbey Island fault zone, and the Devils Mountain fault zones, are modeled in this study as single active faults in the Puget Lowland are. (already covered).

Regional Deformation Considerations

Model block motions agree with geologic constraints and paleomagnetic models (Wells and Simpson, 2001; Wells and Weaver, 1993; Wells et al., 1996). Northward fore-arc migration of about 6 mm per year agrees with and improves upon previous estimates (Mazzotti et al., 2002; Miller et al., 2001; Wells and Johnson, 2000).

Modeled Faults

Seattle Fault Zone

Recent study of the Seattle fault zone (Blakely et al., 2002; Brocher et al., 2001; Brocher et al., 1999b; Calvert and Fisher, 2001; Johnson et al., 1994a; ten Brink et al., 2002) suggests that it is part of a regional, north-directed, thrust system that underlies much of Puget Sound, with slip distributed across a 4 to 6 km-wide zone of one to four south-dipping reverse faults. Modeled dips range from 25° to 60° to the south and slip rate estimates across the active northernmost fault strand range from 0.25 to 1.1 mm per year (Johnson et al., 1999; Pratt et al., 1997).

Here, the Seattle fault is modeled as a single active fault with three segments, extending 85 km along strike (Figure 3), similar to the deformation front modeled by Blakely et al. (2002). The model fault dips 40° to the south and is locked to 15 km depth. Several permanent GPS stations are located within 20 km of the model fault, and thus are sensitive to near-fault elastic effects. Inversion shows 4.5 to 4.9 mm/yr of right lateral strike-slip motion and 1.8 to 3.3 mm/yr of extension <<the way this is presented is confusing…. If it's shortening or extension, omit the "dip slip" which has both a shortening and uplift component). Strike-slip motion is similar in magnitude to that calculated for the flanking Tacoma and South Whidbey Island fault zones. In the GPS velocity field, the block to the north of the Seattle fault has greater northward velocity than the block to the south (Figure 3), perhaps implying extension across the Seattle fault during the GPS observation interval. This is inconsistent with uplift of the southerly hanging wall and well-established evidence for regional contraction. The two GPS stations on the block to the north of the Seattle fault are close together, however, and do not provide a robust geometry for determining block motion. In addition, despite the short distance between them, the two stations are not in good agreement. While proximity to the Seattle fault may contribute differentially to the interseismic strain accumulation at SEAT, neither SEAT nor SEAW is on a geodetic monument and non-tectonic motions may also be a factor.

Tacoma Fault Zone

The south-vergent Tacoma fault zone was recognized in high-resolution marine seismic-reflection data collected as part of the SHIPS project (Brocher et al., 2001; Brocher et al., 1999a). SHIPS tomography images an arcuate structure extending from just north of Tacoma westward across the Kitsap Peninsula, juxtaposing Eocene basalt against younger sedimentary units (Brocher et al., 2001). Structural relief is inferred to increase to a maximum of 6 or 7 km in the west, based on the increased depth of the Tacoma basin. Brocher et al. (2001) suggest that the increased structural relief, together with evidence for coseismic uplift, indicate Holocene activity. Sherrod (1998) notes that vertical uplift of more than 3 m near the western end of the

Tacoma fault zone occurred at about the same time as the last rupture along the Seattle fault zone, around A.D. 900, and likely records south-vergent slip. While a number of fault strands may be present in a fault zone perhaps 8 km in width, individual fault strands have not yet been resolved (Brocher et al., 2001).

The Tacoma fault zone is modeled here as a single active fault with three segments, extending 95 km along strike (Figure 3). The model fault dips 65° to the north and is locked to 15 km depth. Two permanent GPS stations lie within 20 km of the fault. The model fault corresponds reasonably well with that of Brocher et al. (2001), although the model fault is extended eastward to the Coast Range Boundary fault in order to satisfy polygon closure requirements of the block model. Inversion calculates 4.0 to 5.0 mm/yr of right lateral strike-slip motion and 0.1 to 3.9 mm/yr of reverse dip-slip motion (horizontal component). No previous dip-slip rates have been estimated for the Tacoma fault.

South Whidbey Island Fault Zone

Relatively little is known about the South Whidbey Island fault zone, which separates the Seattle basin from the Everett basin to the north. Magnetic and gravity anomalies, as well as offsets of Quaternary stratigraphy observed in drill holes, indicate a large unexposed fault (Gower et al., 1985). The Coast Range Boundary fault, forming the eastern margin of the Tacoma and Seattle basins, extends to the trace of the northwest-striking South Whidbey Island fault zone (Clowes et al., 1987; Johnson, 1984; Johnson et al., 1994b). To the northwest, near Vancouver Island, the South Whidbey Island fault zone merges with the Devils Mountain fault zone. The South Whidbey Island fault zone forms the boundary between mafic submarine volcanic rocks of the Eocene Crescent Formation to the southwest and a diverse assemblage of pre-Tertiary rocks to the northeast (Johnson et al., 1996). Thick Quaternary sediments bury the downthrown block and obscure the contact between these two blocks. Industry seismic-reflection profiles and displacement along exposed faults in Quaternary sediments reasonably constrain location of the fault zone.

Johnson et al. (1996) modeled a fault zone ranging from 6 to 11 km in width, with at least three strands dipping steeply to the north, and dominated by right lateral strike-slip. Industry boreholes adjacent to the fault zone indicate about 420 m of structural relief on the Quaternary–Tertiary boundary, which is inferred to be displacement due to reverse fault slip. If correct, this displacement suggests a reverse slip rate of about 0.2 mm per year during the last 1.8 million years. Based on offsets mapped in Pleistocene deposits, Johnson et al. (1996) interpret a minimum Quaternary uplift rate of 0.6 mm per year and suggest that the rate could be considerably higher. Since the fault strands are sub-vertical, the uplift rate is essentially the same as the dip-slip rate.

In this study, the South Whidbey Island fault zone is modeled as a single active fault with five segments, extending northwesterly across Puget Sound for about 175 km (Figure 3). The model fault dips 80° to the north and the locking depth is assumed to be 15 km. One GPS station is located within 20 km of the model fault. The model fault location and orientation compare reasonably well with the evaluation by Johnson et al. (1996). Inversion results in contraction ranging from 1.8 mm per year of normal motion along the southeast portion of the fault to 4.5

mm per year of reverse motion along the fault towards the northwest. Strike-slip motion is left lateral and ranges from 4.5 to 6.3 mm per year.

Devils Mountain Fault Zone

The Devils Mountain fault zone extends 125 km from the Cascade Range foothills to Vancouver Islandforming the northern boundary of the Quaternary Bellingham basin and separating thrust-imbricated Paleozoic and Mesozoic volcanic and associated clastic rocks to the northeast (Tabor, 1994) from Mesozoic clastic marine fan and oceanic melange units to the southwest, accreted to the continent during Early Cretaceous time (Brown et al., 1987; Tabor, 1994). Right lateral strike-slip is suggested before the early Oligocene when intrusive stocks annealed the eastern portion of the fault. Other workers concluded that strike-slip was left lateral (Evans and Ristow, 1994; Lovseth, 1975; Whetten, 1978). Based partly on seismic reflection imaging, the Devils Mountain fault zone has been more recently interpreted as an active left lateral, oblique-slip, transpressional master fault dipping 45° to 75° to the north (Johnson et al., 2001). Northwest-striking *en echelon* folds and faults border the main fault strand (Johnson et al., 2001). To the southeast, the Devils Mountain fault zone merges with the Straight Creek fault. The Straight Creek and Devils Mountain faults most likely underwent synchronous movement in late middle Eocene to early Oligocene time. To the west, the Devils Mountain fault zone may merge with the South Whidbey Island fault zone and ultimately with the Leech River fault on Vancouver Island (Mosher and Rathwell, 2000).

Based on subsurface data, offsets of glaciomarine features, and marine high-resolution seismic-reflection data, the late Pleistocene reverse dip-slip rate for the master Devils Mountain fault zone ranges from 0.05 to 0.31 mm per year (Johnson et al., 2001). Estimated slip rates for some of the *en echelon* fault strands are comparable. Johnson et al. (2001) suggest that the Devils Mountain fault zone may have undergone left lateral strike-slip at a rate of 0.75 mm per year since late middle Eocene time.

The Devils Mountain fault zone is modeled here as a single active structure composed of eleven segments (Figure 3), extending approximately 170 km across the Strait of Juan de Fuca to join the Leech River fault. The model fault dips 61° to the north and the seismogenic depth is assumed to be 15 km. Several permanent GPS stations are located within 20 km of the fault zone. Inversion resulted in relatively uniform right lateral strike-slip rates along the main portion of the fault, ranging from 1.2 to 1.7 mm per year. Dip-slip rates (horizontal component) from inversion range from 1.2 mm to 9.1 mm per year of reverse motion, increasing in magnitude towards the west. The fault segment that connects the Devils Mountain fault zone and the South Whidbey Island fault zone to the Leech River fault on Vancouver Island shows 0.8 mm per year of reverse dip-slip (horizontal component) and 0.3 mm per year of right lateral strike-slip.

Leech River Fault

The Leech River fault on southern Vancouver Island separates the Siletz terrane, a thick slab of lower Eocene oceanic crust and overlying marine clastic sediments, from the pre-Tertiary rocks of Pacific Rim terrane and the superjacent Wrangellia terrane to the north (Figure 5). The Pacific Rim terrane comprises metasedimentary rocks accreted to the continental margin in earliest Eocene time. Wrangellia terrane accreted to the continent in middle Cretaceous time and consists of mafic volcanic rocks capped with shallow marine shale and interbedded limestone (Brandon et al., 1998). The Leech River fault is clearly imaged in high-resolution seismic-reflection surveys and dips about 30° to the north (Clowes et al., 1987). Although many earthquake epicenters are found along the surface trace of the fault, hypocenters are not located along the subsurface trace of the fault (Mulder and Rogers, 2002) and may instead reflect regional tectonic stress in underlying Crescent/Metchosin basalts. Conglomerates shed southward from uplifted pre-Tertiary rocks north of the Leech River fault indicate the fault may have been active in late Eocene time (Brandon et al., 1998). Cross-cutting relationships limit accretion of Pacific Rim terrane along the Leech River suture to between middle Eocene time and late Oligocene time (Brandon and Vance, 1992). <<any geologic evidence of its current activity?>>

The Leech River fault is here modeled as a single active fault consisting of one segment, extending 42 km across southern Vancouver Island (Figure 3, Figure 10). The model fault dips 30° to the north and the seismogenic depth is assumed to be 15 km. No CGPS stations are located within 20 km of the fault. The model fault location and length fit well with a prominent linear feature evident on a digital elevation model (Haugerud, 1999). The modeled dip is taken from a Lithoprobe transect (Clowes et al., 1987). The model indicates 0.2±0.1 mm/a right lateral strike-slip, together with 0.2 mm±0.1 per year of contraction.

Little River Fault

The locus of deformation along the north and northeastern margins of the Olympic Mountains (Figure 3) is obscure. An accretionary wedge formed inboard of the Cascadia megathrust underlies much of the continental shelf; on land, the older, Olympic accretionary complex forms the uplifted core of the Olympic Mountains (Brandon et al., 1998). Detailed LIDAR topography shows a 30-km long, west-northwest-striking Holocene fault scarp along the north side of the Olympic Peninsula (Haugerud, 2002). The fault scarp offsets late Pleistocene glacial features and may offset younger landslides. Regional mapping indicates the presence of more than one large scale fault trace in this area (Harris, 1998). It has been suggested that the Little River fault might accommodate both right lateral strike-slip as well as shortening due to coseismic westward escape of the Olympic Mountains block (Haugerud, 2002).

In this study, the Little River fault is inferred to extend to the west where it merges with the Tofino fault offshore from Vancouver Island and to the east where it terminates against the Hood Canal fault, a distance of about 220 km (Figure 3). The fault is modeled with nine segments, all dipping 70° to the north or northeast. The locking depth is assumed to be 15 km. One GPS station (BLYN) is located within a kilometer or so of model fault. The relatively steep model dip is consistent with dips on the north limb of the Hurricane Ridge fault located a short distance to the south (Brandon et al., 1998). Right lateral strike-slip rates from inversion range from 3.8 to 4.5 mm per year, with 1σ uncertainty ranging from 0.4 to 1.9 mm per year. Shortening rates range from -2.1 mm per year (extension) to 1.4 mm per year contraction, with 1σ uncertainty ranging from 0.1 to 0.2 mm per year. The normal dip-slip rates are calculated for segments where the model fault strikes more towards the north and are likely artifacts of model geometry.

Doty Fault

The west-striking Doty fault is located in the Puget Lowland of southwestern Washington about 125 km south of Seattle and its importance has only recently been recognized. Although the fault is noted in passing on a number of U.S. Geological Survey compilation maps (e.g., Brocher et al. [2001]), the only published description of the fault is found in Wong et al. (2000). That study indicates the Doty fault is 65 km long, dips 70° to the north, and has a dip-slip rate ranging from 0.2 to 0.5 mm per year. In order to meet model requirements, the model Doty fault was speculatively extended both east and west of the Puget Lowland (Walsh et al., 1999).

In this study, the model Doty fault extends across the southern Puget Lowland and offshore to the Cascadia megathrust, a distance of about 230 km (Figure 3). The fault is modeled with a dip of 70° to the north and the seismogenic depth is assumed to be 15 km. No GPS stations are within 20 km of the model fault. The eastern portion of the model fault location reasonably fits mapped faults in the area (Walsh et al., 1999). Extending the fault towards the west is required for block closure and is structurally plausible, although the fault location is poorly constrained by geology or geophysics. Model strike-slip rates on the model Doty fault are left lateral, ranging from 0.2 to 1.3 mm per year, with 1σ uncertainty of 0.1 mm per year. Model dip-slip rates along the Doty fault range from 0 to 4.6 mm per year (horizontal component), with 1σ uncertainty of 0.1 mm per year. Dip-slip rates increase systematically towards the west, perhaps indicating block rotation.

Seismic Hazard Considerations

The kinematic model yields estimates of block motions that collectively make up the regional deformation budget and set limits on seismogenic strain accumulation. Taken with specific fault geometry, dip, and locking depth, these yield limits on earthquake frequency and magnitude, and yield first order constraints of the seismic moment accumulating in the region are possible, although not all recoverable deformation is seismically released (e.g., Dragert, Miller, etcl). Moment magnitude calculations are based on the assumptions that faults lock and accumulate energy, that dip and locking depths are reasonably well known, and all recoverable strain is seismically released during rupture. Moment magnitude calculations require an estimate of the size of the locked area or patch for each fault and the annual slip rate for each fault. Inverted block motions and model fault geometry yield slip rates that are applied to a finite fault patch with a surface strike length, dip, and the seismogenic depth. Moment magnitude estimates use the formula:

$$M_w = 2/3 * \log_{10} M_o - 10.7$$

where M_o is the seismic moment in dyne-cm (Hanks and Kanamori, 1979; Kanamori, 1977), calculated using the formula $M_o = \mu DA$ where μ is the shear modulus, D is the annualized displacement and A is the area of slip on the fault.

If the limiting magnitude of an earthquake is assumed, earthquake recharge intervals for individual faults can be calculated from estimated slip rates. In the following calculations, four different alternatives are considered; maximum patch rupture earthquakes of M_w 6 and M_w 7, and 50% patch rupture earthquakes of M_w 6 and M_w 7. Due to uncertainties related to the Doty fault, 50% and 25% of the maximum fault length represent conservative rupture scenarios for this fault. Fault slip rates employed in these calculations are the total slip rates in the plane of the fault along individual faults (vector sum of the dip-slip and strike-slip rates). The amount of slip required to produce M_w 6 and M_w 7 earthquakes on each fault, assuming a maximum patch rupture, is shown in Table 6:

Table 6. Slip Amount and Earthquake Recharge Intervals for M_w 6 and M_w 7 Earthquakes (100% rupture patch)

Fault	***Required slip for rupture (m)***	***Length (km)***	***Locking depth (km)***	***Dip***	***Slip vector (from inversion) (mm/year)***	***Recharge interval (years)***
M_w = 6						
Seattle	0.016	85	15	40°S	5.60	3
Doty[(1)]	0.016	115	15	70°N	9.54	2
Tacoma	0.020	95	15	65°N	5.57	3
S. Whidbey[(2)]	0.014	145	15	80°N	4.93	3
Devils Mtn[(3)]	0.015	120	15	61°N	7.75	2
M_w = 7						
Seattle	0.480	85	15	40°S	5.60	86
Doty[(1)]	0.520	115	15	70°N	9.54	55
Tacoma	0.610	95	15	65°N	5.57	109
S. Whidbey[(2)]	0.430	145	15	80°N	4.93	87
Devils Mtn[(3)]	0.460	120	15	61°N	7.75	59

[(1)] 50% rupture patch, excluding 3 eastern segments of Doty fault
[(2)] excluding the westernmost segment of the S. Whidbey Island fault
[(3)] excluding three eastern segments of the Devils Mountain fault

<<Are these broadly consistent with frequency-magnitude relationships and magnitude-strike-length scaling?

Similar calculations can be made for scenarios in which 50% of the maximum patch area ruptures. Required slip and earthquake recharge intervals for M_w 6 and M_w 7 earthquakes for this case are shown in Table 7:

Table 7. Slip Amount and Earthquake Recharge Intervals for M_w 6 and M_w 7 Earthquakes (50% rupture patch)

Fault	***Required slip for rupture (m)***	***Length (km)***	***Locking depth (km)***	***Dip***	***Slip vector (from inversion) (mm)***	***Recharge interval (years)***
M_w 6						
Seattle	0.031	42.5	7.5	40°S	5.60	6
Doty[(1)]	0.033	115	7.5	70°N	9.54	3
Tacoma	0.038	47.5	7.5	65°N	5.57	7
S. Whidbey[(2)]	0.027	72.5	7.5	80°N	4.93	5

Devils Mtn.[3]	0.029	120	7.5	61°N	7.75	4
M_w 7						
Seattle	0.980	85	7.5	40°S	5.60	175
Doty[1]	1.050	115	7.5	70°N	9.54	110
Tacoma	1.200	95	7.5	65°N	5.57	215
S. Whidbey[2]	0.860	145	7.5	80°N	4.93	174
Devils Mtn.[3]	0.920	120	7.5	61°N	7.75	119

(1) 25% rupture patch, excluding 3 eastern segments of Doty fault
(2) excluding the westernmost segment of the S. Whidbey Island fault
(3) excluding three eastern segments of the Devils Mountain fault

A number of factors may impact earthquake recharge interval or moment accumulation calculations. For example, seismogenic depths in the Puget Lowland are poorly constrained and may be somewhat greater or less than the assumed 15 km. While this may have little impact on block motions calculated from inversion, increasing or decreasing the size of the locked patch has implications for seismic moment accumulation, required slip, and recharge interval calculations. Increasing seismogenic depth or decreasing fault dip, for example, would increase the fault rupture area and thus decrease the amount of required slip for an earthquake of given size. This would consequently decrease the recharge interval for a fixed magnitude earthquake as the annual moment accumulation increases.

An alternative approach to calculating earthquake recharge intervals is to consider annual moment accumulation and the amount of moment released during earthquakes. For each the four major faults in the Puget Sound area (Tacoma, Seattle, South Whidbey Island and Devils Mountain faults), annual moment accumulations were calculated for a maximum fault patch where seismogenic strain accumulates over 100% of the length of the fault trace down to the seismogenic depth, as well as for a possibly more realistic case in which only 50% of the maximum patch accumulates seismogenic strain. Because about 85% of accumulated seismic moment is released by earthquakes with magnitude equal to or greater than M_w 7 (Stein and Hanks, 1998), moment release can be regarded as depending almost entirely on earthquakes with magnitudes greater than M_w 6. In the Puget Sound area, only one crustal earthquake greater than M_w 6 is known from the paleoseismic record or from seismic recordings. The >M_w 7 earthquake of about 900 A.D. along the Seattle fault is the only presently known crustal rupture in the Puget Sound area that was of sufficient magnitude to release a large amount of accumulated moment. Although the actual moment magnitude of this earthquake is unknown, M_w 7 is viewed as a conservative estimate. For an earthquake along the Seattle fault, assuming the seismogenic depth is 15 km, a 40-km long rupture requires an average slip of 1.3 meters in order to produce a M_w 7 event. The moment released under these conditions is 4.00×10^{26} dyne-cm. For a hypothetical M_w 6 earthquake on the same fault, the moment release would be 1.26×10^{25} dyne-cm. Annual moment magnitude accumulation for the maximum (100%) patch case and the 50% patch case, together with recharge intervals based on release of M_w 6 or M_w 7 earthquakes, assuming that all accumulated moment is released by rupture on individual faults, are shown in Table 9:

Table 9. Earthquake Recharge Intervals from Moment Accumulation

Considerations

Fault	*Slip vector (from inversion) (mm/year)*	*Length (km)*	*Locking depth (km)*	*Annual moment accumulation (dyne-cm)*	*Recharge interval[(1)] (years)*	*Recharge interval[(2)] (years)*
100% patch rupture					***M_w 6***	***M_w 7***
Seattle	5.60	85	15	3.67E+24	3	109
Tacoma	5.75	95	15	2.89E+24	4	139
S. Whidbey[(3)]	4.93	145	15	3.59E+24	4	111
Devils Mtn[(4)]	7.75	120	15	5.26E+24	2	76
50% patch rupture					***M_w 6***	***M_w 7***
Seattle	5.60	42.5	15	1.83E+24	21	655
Tacoma	5.75	47.5	15	1.45E+24	22	687
S. Whidbey[(3)]	4.93	72.5	15	1.80E+24	21	669
Devils Mtn[(4)]	7.75	60	15	2.63E+24	11	363

(1) based on moment release in M_w 6 earthquake of 1.26 x 10^{25} dyne-cm
(2) based on moment release in M_w 7 earthquake of 4.00 x 10^{26} dyne-dm
(3) excluding the westernmost segment of the S. Whidbey Island fault
(4) excluding three eastern segments and western segment of the Devils Mountain fault

Earthquake recharge intervals calculated from moment accumulation considerations for the 50% patch rupture case are compared with recharge intervals calculated from slip rates for 50% patch rupture in Table 10:

Table 10. Earthquake Recharge Interval Comparison

Fault	*Recharge intervals from slip rates*	*Recharge intervals from moment accumulation*
	M_w 6	***M_w 6***
Seattle	6	21
Tacoma	7	22
S. Whidbey	5	21
Devils Mtn	4	11
	M_w 7	***M_w 7***
Seattle	175	655
Tacoma	215	687
S. Whidbey	175	669
Devils Mtn	119	363

By either method, if accumulated slip or moment were released by M_w 6 earthquakes, the earthquake recharge interval for key crustal faults in Puget Sound should be about ten to twenty years and about 100 to about 650 years for M_w 7 earthquakes. Since the most recent large earthquake in the Puget Sound area occurred 1,100 years ago (Bucknam et al., 1992), these recharge estimates suggest a deficit of M_w 6 earthquakes, as well as a possible deficit of larger

M_w 7 earthquakes on the key crustal faults. This apparent seismicity deficit may be in part related to an incomplete earthquake catalog for the Puget Sound area, where the historic catalog is 150 years and paleoseismic events are obscured by a Holocene landscape. Another possibility is that most accumulated strain in the Puget Sound area is released by M_w 7 or larger earthquakes, and smaller M^w 6 earthquakes do not typically occur. Alternatively, earthquakes in the Puget Sound area may be clustered or grouped in time, with the historic interval representing a period of relative quiescence and the Holocene landscape providing a poor record of real events.

Stress drops were also calculated for possible M_w 7 and M_w 6 earthquakes on the Doty, Tacoma, Seattle, South Whidbey Island and Devils Mountain faults, using the formula $\Delta\sigma \approx (2\mu D)/w$ where μ is the shear modulus, D is the average displacement, and w is the width of the fault (Shearer, 1999). All calculations assume rupture to a locking depth of 15 km and the displacements used were those required to generate an earthquake of the specified magnitude over the rupture patch (Table 6 and Table 7). For a 100% rupture patch, stress drops for an M_w 7 earthquake range from 13.6 to 40.3 bars, and for an M_w 6 earthquake from 0.5 to 1.3 bars. Similar calculations for the 50% rupture patch case results in stress drops of 27.7 to 79.2 bars for an M_w 7 earthquake and 0.9 to 2.5 bars for an M_w 6 earthquake. Since observed stress drops are usually in the range of 10 to 100 bars (Shearer, 1999), these stress drops are reasonable for M_w 7 earthquakes but are too small for M_w 6 earthquakes on faults in Puget Sound. These stress drop considerations, as well as the empirical scaling relationships of Wells and Coppersmith (1992), suggest that M_w 6 rupture is unlikely to occur over the entire length of active faults in the Puget Sound area.

The historic earthquake record for Washington State contains no crustal earthquakes larger than M_w 6 in the past 150 years in the Puget Lowland. Geodetic data supporting fault slip and geologic data supporting seismogenic strain release support the inferred deficit in regional shallow seismicity.

CONCLUSIONS

Calculated slip from an inversion constrained by the PANGA CGPS velocity field across a crustal block model supports the interpretation that the Cascadia forearc is translating northward, with shortening due to buttressing against relatively immobile crystalline fore-arc to the north. North-south directed horizontal shortening estimates from inversion, with improved precision over previous estimates, are 6.2 ± 1.0 mm per year across the Puget Lowland and 6.1 ± 0.3 mm per year across the foreland to the west (Table 5). This is comparable to north-directed shortening of approximately 8 mm per year in metropolitan Los Angeles, where shortening is buttressed against the southern San Gabriel Mountains (Argus et al., 1999). There, vertical thickening along a fold and thrust belt accommodate north-south contraction, with concomitant east to west extension and conjugate strike-slip faulting. In the Puget Lowland, West- to west-northwest-striking reverse faults accommodate vertical thickening; west-northwest-striking faults such as the Devils Mountain and Little River accommodate strike-slip. Argus et al. (1999) estimate <0.25 mm per year east to west lengthening across metropolitan Los Angeles. The east to west lengthening rate across northern Puget Sound and the Olympic Peninsula (Figure 3) is greater at about 3 mm per year. This rate decreases towards the south, where east to west lengthening on the north side of the Doty fault is <0.9 mm per year.

Estimated earthquake recharge intervals for several key faults in the Puget Lowland, based on slip rates and moment accumulation considerations, range from 2 to 22 years for M_w 6 earthquakes and from 55 to 687 years for M_w 7 earthquakes. These estimates, together with stress drop considerations, indicate that too few M_w 6 or larger earthquakes have occurred within the past 150 years to account for the strain accumulation determined by GPS geodesy. Although this deficit may be related in part to temporal clustering of earthquakes, the earthquake catalog is not complete enough or sufficiently long to test this hypothesis. In addition, accumulated strain may be typically released by earthquakes of M_w 7 or larger, with little strain release by smaller ruptures.

REFERENCES

Atamimi, Z., Sillard, P., and Boucher, C., 2002, ITRF2000: A new release of the International Terrestrial Reference Frame for earth science applications: Journal of Geophysical Research, v. 107, no. B10, p. 2214.

Argus, D. F., Heflin, M. B., Donnellan, A., Webb, F. H., Dong, D., Hurst, K. J., Jefferson, D. C., Lyzenga, G. A., Watkins, M. M., and Zumberge, J. F., 1999, Shortening and thickening of metropolitan Los Angeles measured and inferred by using geodesy: Geology, v. 27, no. 8, p. 703-706.

Blakely, R. J., Wells, R. E., Weaver, C. S., and Johnson, S. Y., 2002, Location, structure, and seismicity of the Seattle fault zone, Washington; evidence from aeromagnetic anomalies, geologic mapping, and seismic-reflection data: Geological Society of America Bulletin, v. 114, no. 2, p. 169-177.

Blewitt, G., Lavallee, D., Clarke, P., and Nurutdinov, K., 2001, A new global mode of Earth deformation; seasonal cycle detected: Science, v. 294, no. 5550, p. 2342-2345.

Bourgeois, J., and Johnson, S. Y., 2001, Geologic evidence of earthquakes at the Snohomish Delta, Washington, in the past 1200 yr: Geological Society of America Bulletin, v. 113, no. 4, p. 482-494.

Brandon, M. T., Roden-Tice, M. K., and Garver, J. I., 1998, Late Cenozoic exhumation of the Cascadia accretionary wedge in the Olympic Mountains, Northwest Washington State: Geological Society of America Bulletin, v. 110, no. 8, p. 985-1009.

Brandon, M. T., and Vance, J. A., 1992, Tectonic evolution of the Cenozoic Olympic subduction complex, Washington State, as deduced from fission track ages for detrital zircons: American Journal of Science, v. 292, no. 8, p. 565-636.

Brocher, T. M., Parsons, T., Blakely, R. J., Christensen, N. I., Fisher, M. A., Wells, R. E., ten Brink, U. S., Pratt, T. L., Crosson, R. S., Creager, K. C., Symons, N. P., Preston, L. A., Van Wagoner, T., Miller, K. C., Snelson, C. M., Trehu, A. M., Langenheim, V. E., Spence, G. D., Ramachandran, K., Hyndman, R. A., Mosher, D. C., Zelt, B. C., and Weaver, C. S., 2001, Upper crustal structure in Puget Lowland, Washington; results from the 1998 seismic hazards investigation in Puget Sound: Journal of Geophysical Research, B, Solid Earth and Planets, v. 106, no. 7, p. 13,541-13,564.

Brocher, T. M., Parsons, T. E., Creager, K. C., Crosson, R. S., Symons, N. P., Spence, G. D., Zelt, B. C., Hammer, P. T., Hyndman, R. D., Mosher, D. C., Trehu, A. M., Miller, K. C., ten Brink, U. S., Fisher, M. A., Pratt, T. L., Alvarez, M. G., Beaudoin, B. C., Louden, K. E., and Weaver, C. S., 1999a, Wide-angle seismic recordings from the 1998 Seismic Hazards Investigation of Puget Sound (SHIPS), western Washington and British Columbia: U.S. Geological Survey Open File Report 99-0314, 110 p.

Brocher, T. M., Parsons, T. E., Fisher, M. A., Blakely, R. J., ten Brink, U. S., Creager, K. C., Crosson, R. S., Miller, K. C., Trehu, A. M., Spence, G., Zelt, B. C., Hyndman, R. D., and Mosher, D. C., 2000, Internal structure of Cenozoic basins in the Puget Lowland, Washington; results from SHIPS, the 1998 Seismic Hazards Investigation in Puget Sound: Geological Society of America, Cordilleran Section, 96th annual meeting Abstracts with Programs - Geological Society of America, v. 32, no. 6, p. 6.

Brocher, T. M., Parsons, T. E., Fisher, M. A., ten Brink, U. S., Molzer, P. C., Creager, K. C., Crosson, R. S., Trehu, A. M., Miller, K. C., Pratt, T. L., and Weaver, C. S., 1999b, Structure of the Seattle Basin; a tomographic model using data from the 1998 seismic hazards investigation in Puget Sound (SHIPS) experiment, Washington State: SSA-99 94th annual meeting; meeting abstracts Seismological Research Letters, v. 70, no. 2, p. 219.

Brown, E. H., Blackwell, D. L., Christenson, B. W., Frasse, F. I., Haugerud, R. A., Jones, J. T., Leiggi, P. A., Morrison, M. L., Rady, P. M., Reller, G. J., Sevigny, J. H., Silverberg, D. S., Smith, M. T., Sondergaard, J. N., and Ziegler, C. B., 1987, Geologic map of the Northwest Cascades, Washington: Geological Society of America Map and Chart Series 61.

Bucknam, R. C., Hemphill-Haley, E., and Leopold, E. B., 1992, Abrupt uplift within the past 1,700 years at southern Puget Sound, Washington: Science, v. 258, p. 1611-1614.

Bucknam, R. C., Perkins, D. M., and Sherrod, B. L., 1997, Developing quantitative seismic hazard information from incomplete paleoseismic records; examples from the Puget Sound region, Washington: Geological Society of America, 1997 annual meeting Abstracts with Programs - Geological Society of America, v. 29, no. 6, p. 131.

Calvert, A. J., and Fisher, M. A., 2001, Imaging the Seattle fault zone with high-resolution seismic tomography: Geophysical Research Letters, v. 28, no. 12, p. 2337-2340.

Caron, M. E., 2003, Realization of Continuous GPS Velocities Over an Active Crustal Block Model for the Puget Sound Area and the Implications for Seismic Hazard [Masters thesis]: Central Washington University, 92 p.

Clowes, R. M., Brandon, M. T., Green, A. G., Yorath, C. J., Brown, A. S., Kanasewich, E. R., and Spencer, C., 1987, Lithoprobe, southern Vancouver Island; Cenozoic subduction complex imaged by deep seismic reflections: Canadian Journal of Earth Sciences = Journal Canadien des Sciences de la Terre, v. 24, no. 1, p. 31-51.

DeMets, C., and Dixon, T. H., 1999, New kinematic models for Pacific-North America motion from 3 Ma to present; I, Evidence for steady motion and biases in the NUVEL-1A model: Geophysical Research Letters, v. 26, no. 13, p. 1921-1924.

DeMets, C., Gordon, R. G., Argus, D. F., and Stein, S., 1994, Effect of recent revisions to the geomagnetic reversal time scale on estimates of current plate motions: Geophysical Research Letters, v. 21, no. 20, p. 2191-2194.

Easterbrook, D. J., 1992, Advance and retreat of Cordilleran ice sheets in Washington, U.S.A: Geographie Physique et Quaternaire, v. 46, no. 1, p. 51-68.

Evans, J. E., and Ristow, R. J., Jr., 1994, Depositional history of the southeastern outcrop belt of the Chuckanut Formation; implications for the Darrington-Devil's Mountain and Straight Creek fault zones, Washington (U.S.A.): Canadian Journal of Earth Sciences = Journal Canadien des Sciences de la Terre, v. 31, no. 12, p. 1727-1743.

Fluck, P., Hyndman, R. D., and Wang, K., 1997, Three-dimensional dislocation model for great earthquakes of the Cascadia subduction zone: Journal of Geophysical Research, B, Solid Earth and Planets, v. 102, no. 9, p. 20,539-20,550.

Gower, H. D., Yount, J. C., and Crosson, R. S., 1985, Seismotectonic map of the Puget Sound region, Washington: U.S. Geological Survey Miscellaneous Investigations Series Map GP-988.

Hanks, T. C., and Kanamori, H., 1979, A moment magnitude scale: Journal of Geophysical Research, v. 84, no. B5, p. 2348-2350.

Harris, C. F. T., 1998, 1-100,000-Scale Digital Geology of Washington State, Digital Report 2: Washington State Department of Natural Resources, Division of Geology and Earth Resources v. 1, scale 1:100,000.

Haugerud, R. A., 2002, Lidar Evidence for Holocene Surface Rupture on the Little River Fault near Port Angeles, Washington: Seismological Research Letters, v. 73, no. 2, p. 248.

Haugerud, R. A., comp., 1999, Digital elevation model (DEM) of Cascadia, latitude 39N-53N, longitude 116W-133W, U.S. Geological Survey Open File 99-0369.

Johnson, S. Y., 1984, Evidence for a margin-truncating transcurrent fault (pre-late Eocene) in western Washington: Geology (Boulder), v. 12, no. 9, p. 538-541.

Johnson, S. Y., Dadisman, S. V., Childs, J. R., and Stanley, W. D., 1999, Active tectonics of the Seattle Fault and central Puget Sound, Washington; implications for earthquake hazards: Geological Society of America Bulletin, v. 111, no. 7, p. 1042-1053.

Johnson, S. Y., Dadisman, S. V., Mosher, D. C., Blakely, R. J., and Childs, J. R., 2000, Late Quaternary tectonics of the Devils Mountain Fault and related structures, northern Puget Lowland: Geological Society of America, Cordilleran Section and associated societies, 96th annual meeting; Abstracts with Programs - Geological Society of America, v. 32, no. 6, p. 21.

-, 2001, Active tectonics of the Devils Mountain Fault and related structures, northern Puget Lowland and eastern Strait of Juan de Fuca region, Pacific Northwest: U.S. Geological Survey Professional Paper 1643.

Johnson, S. Y., Potter, C. J., and Armentrout, J. M., 1994a, Origin and evolution of the Seattle Fault and Seattle Basin, Washington: Geology (Boulder), v. 22, no. 1, p. 71-74.

Johnson, S. Y., Potter, C. J., Armentrout, J. M., Finn, C., and Weaver, C. S., 1994b, The southern Whidbey Island Fault, Puget Lowland, Washington: Geological Society of America, 1994 annual meeting Abstracts with Programs - Geological Society of America, v. 26, no. 7, p. 188.

Johnson, S. Y., Potter, C. J., Armentrout, J. M., Miller, J. J., Finn, C. A., and Weaver, C. S., 1996, The southern Whidbey Island Fault; an active structure in the Puget Lowland, Washington: Geological Society of America Bulletin, v. 108, no. 3, p. 334-354.

Kanamori, H., 1977, The energy release in great earthquakes: Journal of Geophysical Research, v. 82, p. 2981-2987.

Karlin, R. E., Naugler, W. E., and Holmes, M. L., 1995, Extensive submarine landslides in Puget Sound and Lake Washington; implications for recurrence intervals of large earthquakes in the Pacific Northwest: Geological Society of America, 1995 annual meeting Abstracts with Programs - Geological Society of America, v. 27, no. 6, p. 429-430.

Lovseth, T. P., 1975, The Devils Mountain fault zone, northwestern Washington [Master's thesis]: University of Washington, Seattle, 29 p.

Mazzotti, S., Dragert, H., Hyndman, R. D., Miller, M. M., and Henton, J. A., 2002, GPS deformation in a region of high crustal seismicity; N. Cascadia forearc: Earth and Planetary Science Letters, v. 198, no. 1-2, p. 41-48.

McClusky, S. C., Bjornstad, S. C., Hager, B. H., King, R. W., Meade, B. J., Miller, M. M., Monastero, F. C., and Souter, B. J., 2001, Present day kinematics of the eastern California shear zone from a geodetically constrained block model: Geophysical Research Letters, v. 28, no. 17, p. 3369-3372.

Meade, B. J., Hager, B. H., McClusky, S. C., Reilinger, R. E., Ergintav, S., Lenk, O., Barka, A., and Ozener, H., 2002, Estimates of Seismic Potential in the Marmara

Sea Region from Block Models of Secular Deformation Constrained by Global Positioning System Measurements: Bull. Seis. Soc. Am., v. 92, p. 208-215.

Miller, M. M., Johnson, D. J., Rubin, C. M., Dragert, H., Wang, K., Qamar, A., and Goldfinger, C., 2001, GPS-determination of along-strike variation in Cascadia margin kinematics; implications for relative plate motion, subduction zone coupling, and permanent deformation: Tectonics, v. 20, no. 2, p. 161-176.

Miner, A. M., 2002b, Eocene Tectonics and Active Deformation in Cascadia [Master's thesis]: Central Washington University.

Mosher, D. C., and S.Y. Johnson, eds., and Rathwell, G. J., King, R.B., and Rhea, S.B., comps., 2000, Neotectonics of the eastern Strait of Juan de Fuca; a digital geologic and geophysical atlas: Geological Survey of Canada Open File Report 3931.

Mulder, T. L., and Rogers, G. C., 2002, Seismicity in the vicinity of the Leech River Fault, *in* Seismological Society of America 2002, Annual Meeting 17-19 April 2002, Victoria Conference Centre, Victoria, British Columbia.

Nelson, A. R., Johnson, S. Y., Wells, R. E., Pezzopane, S. K., Kelsey, H. M., Sherrod, B. L., Bradley, L.-A., Koehler, R. D., III, Bucknam, R. C., Haugerud, R., and Laprade, W. T., 2002, Field and laboratory data from an earthquake history study of the Toe Jam Hill Fault, Bainbridge Island, Washington: U.S. Geological Survey Open File Report 02-0060.

Pratt, T. L., Johnson, S. Y., Potter, C. J., Stephenson, W. J., and Finn, C. A., 1997, Seismic reflection images beneath Puget Sound, western Washington State; the Puget Lowland thrust sheet hypothesis: Journal of Geophysical Research, B, Solid Earth and Planets, v. 102, no. 12, p. 27,469-27,489.

Shearer, P. M., 1999, Introduction to Seismology, Cambridge University Press, 260 p.

Sherrod, B. L., 1998, Late Holocene environments and earthquakes in southern Puget Sound [Ph.D. thesis]: University of Washington, Seattle, 159 p.

Stein, R. S., and Hanks, T. C., 1998, M> or =6 earthquakes in southern California during the twentieth century; no evidence for a seismicity or moment deficit: Bulletin of the Seismological Society of America, v. 88, no. 3, p. 635-652.

Tabor, R. W., 1994, Late Mesozoic and possible early Tertiary accretion in western Washington State; the Helena-Haystack melange and the Darrington-Devils Mountain fault zone: Geological Society of America Bulletin, v. 106, no. 2, p. 217-232.

ten Brink, U. S., Molzer, P. C., Fisher, M. A., Blakely, R. J., Bucknam, R. C., Parsons, T., Crosson, R. S., and Creager, K. C., 2002, Subsurface geometry and evolution of the Seattle fault zone and the Seattle Basin, Washington: Bulletin of the Seismological Society of America, v. 92, no. 5, p. 1737-1753.

Thorson, R. M., 1996, Earthquake recurrence and glacial loading in western Washington: Geological Society of America Bulletin, v. 108, no. 9, p. 1182-1191.

Trehu, A. M., Fleming, S. W., Brocher, T. M., Clarke, S. H., Luetgert, J. H., Parsons, T., Meltzer, A. S., and Gulick, S., 1996, Crustal architecture of the Cascadia forearc updated: Geological Society of America, Cordilleran Section, 92nd annual meeting Abstracts with Programs - Geological Society of America, v. 28, no. 5, p. 118.

Walsh, T. J., Korosec, M. A., Phillips, W. M., Logan, R. L., and Schasse, H. W., 1999, Geological map of Washington; southwest quadrant (digital edition): U.S. Geological Survey Open File 99-0382.

Wells, D. L., and Coppersmith, K. J., 1992, Analysis of empirical relationships among magnitude, rupture length, rupture area, and surface displacement: 87th annual meeting of the Seismological Society of America; abstracts Seismological Research Letters, v. 63, no. 1, p. 73.

Wells, R. E., and Johnson, S. Y., 2000, Neotectonics of western Washington and the Puget Lowland resulting from northward migration of the Cascadia forearc: Geological Society of America, Cordilleran Section, 96th annual meeting Abstracts with Programs - Geological Society of America, v. 32, no. 6, p. 75.

Wells, R. E., and Simpson, R. W., 2001, Northward migration of the Cascadia forearc in the northwestern U. S. and implications for subduction deformation: Earth, Planets and Space, v. 53, no. 4, p. 275-283.

Wells, R. E., and Weaver, C. S., 1993, Block deformation in Puget Lowland: U.S. Geological Survey Open File Report 93-0333, p. 14-16.

Wells, R. E., Weaver, C. S., and Blakely, R. J., 1996, Crustal block motions in the Pacific Northwest; implications for the earthquake potential of the Cascadia forearc: Geological Society of America, Cordilleran Section, 92nd annual meeting Abstracts with Programs - Geological Society of America, v. 28, no. 5, p. 123.

Whetten, J. T., 1978, The Devils Mountain Fault; a major Tertiary structure in Northwest Washington: Abstracts with Programs - Geological Society of America, v. 10, no. 3, p. 153.

Wong, I., Silva, W., Bott, J., Wright, D., Thomas, P., Gregor, N., Li, S., Mabey, M., Sojourner, A., and Wang, Y., 2000, Earthquake scenario and probabilistic ground shaking maps for the Portland, Oregon, metropolitan area: Oregon Department of Geology and Mineral Industries Interpretive Map Series No. 16, scale 1:62,500.

Yount, J. C., Dembroff, G. R., and Barats, G. M., 1985, Map showing depth to bedrock in the Seattle 30' by 60' Quadrangle, Washington: U.S. Geological Survey Miscellaneous Field Studies Map MF-1692.

Zumberge, J. F., Heflin, M. B., Jefferson, D. C., Watkins, M. M., and Webb, F. H., 1997, Precise point positioning for the efficient and robust analysis of GPS data from large networks: Journal of Geophysical Research, B, Solid Earth and Planets, v. 102, no. 3, p. 5005-5017.